Original Article

Tumor Biology

Tumor Biology
March 2017: 1–12

DOI: 10.1177/1010428317692261
journals.sagepub.com/home/tub
SAGE

Inhibition of microRNA-21 via locked nucleic acid-anti-miR suppressed metastatic features of colorectal cancer cells through modulation of programmed cell death 4

Reza Nedaeinia[1,2], Mohammadreza Sharifi[3], Amir Avan[4], Mohammad Kazemi[3], Abdolreza Nabinejad[5], Gordon A Ferns[6], Majid Ghayour-Mobarhan[4,7] and Rasoul Salehi[3,8,9]

Abstract

Colorectal cancer is among the most lethal of malignancies, due to its propensity to metastatic spread and multifactorial-chemoresistance. The latter property supports the need to identify novel therapeutic approaches for the treatment of colorectal cancer. MicroRNAs are endogenous non-coding small RNA molecules that function as post-transcriptional regulators of gene expression. Recently, programmed cell death 4 has been identified as a protein that increases during apoptosis. This gene is among the potential targets of miR-21 (OncomiR). Locked nucleic acid–modified oligonucleotides have recently emerged as a potential therapeutic option for targeting microRNAs. The aim of this study was to explore the functional role of locked nucleic acid-anti-miR-21 in the LS174T cell line in vitro and in vivo models. LS174T cells were treated with locked nucleic acid-anti-miR-21 for 24, 48, and 72 h in vitro. The expression of miR-21 and *PDCD4* at messenger RNA (mRNA) level was evaluated by quantitative real-time polymerase chain reaction, while the protein level of *PDCD4* was determined by Western blotting. Cell migratory behavior and the cluster-forming ability of cells were assessed before and after therapy. The disseminated tumor cells were assessed in the chick chorioallantoic membrane model by *Alu* quantitative polymerase chain reaction. Locked nucleic acid-anti-miR-21 was transfected successfully into the LS174T cells and inhibited the expression of miR-21. Locked nucleic acid-anti-miR-21 inhibited the migration and the number of cells forming clusters. Moreover, we found that locked nucleic acid-anti-miR-21 transfection was associated with a significant reduction in metastatic properties as assessed by the in ovo model. Our findings demonstrated the novel therapeutic potential of locked nucleic acid-anti-miR-21 in colon adenocarcinoma with high miR-21 expression.

[1]Department of Medical Biotechnology, School of Medicine, Mashhad University of Medical Sciences, Mashhad, Iran
[2]Students Research Committee, School of Medicine, Mashhad University of Medical Sciences, Mashhad, Iran
[3]Department of Genetics and Molecular Biology, School of Medicine, Isfahan University of Medical Sciences, Isfahan, Iran
[4]Molecular Medicine Group, Department of Modern Sciences and Technologies, School of Medicine, Mashhad University of Medical Sciences, Mashhad, Iran
[5]Isfahan Research Center for Agriculture and Natural Resources, Isfahan, Iran
[6]Division of Medical Education, Brighton and Sussex Medical School, University of Brighton, Brighton, UK
[7]Biochemistry of Nutrition Research Center, School of Medicine, Mashhad University of Medical Sciences, Mashhad, Iran
[8]Acquired Immunodeficiency Research Center, Isfahan University of Medical Sciences, Isfahan, Iran
[9]Gerfa Namayesh Azmayesh (GENAZMA) Science and Research Institute, Isfahan, Iran

Corresponding authors:
Majid Ghayour-Mobarhan, Molecular Medicine Group, Department of Modern Sciences and Technologies, School of Medicine, Mashhad University of Medical Sciences, Mashhad 91778-99191, Iran.
Email: ghayourm@mums.ac.ir

Rasoul Salehi, Department of Genetics and Molecular Biology, School of Medicine, Isfahan University of Medical Sciences, P.O. Box 319, Hezar-Jerib Ave, Isfahan, Iran.
Email: r_salehi@med.mui.ac.ir

Keywords
microRNA-21, colorectal cancer, *PDCD4*, locked nucleic acid-anti-microRNA

Date received: 3 June 2016; accepted: 11 August 2016

Introduction

Colorectal cancer (CRC) is the third leading cause of cancer-related death.[1] The America Cancer Society has predicted that there would be 95,270 cases of colon cancer and 39,220 cases of rectal cancer in 2016 in the United States. Moreover, it is expected that more than 49,190 deaths from CRC will occur in 2016 in the United States.[2] Despite extensive clinical and preclinical developments, the prognosis of CRC is still extremely poor, because of its aggressive properties and its intrinsic resistance to most chemotherapeutic agents.[3] Our data provide a proof of principle for developing a new therapeutic approach and identifying the molecular mechanisms underlying the drug resistance in CRC.

Recently, programmed cell death 4 (*PDCD4*) has been identified as a tumor suppressor gene and is being suggested as a potential therapeutic target. This gene is among the potential targets of microRNA-21 (miR-21), although the molecular mechanism is still obscure.[4] It has been shown that *PDCD4* can interact with several translational factors, including eukaryotic translation initiation factor-4G (*eIF4G*) and eukaryotic translation initiation factor-4A (*eIF4A*), and could suppress translation of mRNA.[5,6] High levels of *PDCD4* may be associated with reduced levels of dUTPase and might contribute to the tumor suppressor function of *PDCD4* in Bon-1 cells.[4] The regulatory role of *PDCD4* is mediated via *P21*,[7] *Cdk4*, ornithine decarboxylase,[8] *carbonic anhydrase II*,[9] *JNK/c-Jun/AP-1*,[5,10] and tissue inhibitor of metalloproteinase 2 (*TIMP-2*).[11] The downregulation of *PDCD4* in lung and colorectal cancers has been found to be associated with a poor prognosis.[12,13]

Chen et al.[14] evaluated the prognostic value of *PDCD4* using two molecular profiling techniques complementary DNA (cDNA) and tissue microarray analysis in 124 patients with primary lung carcinomas. They identified *PDCD4* as a potential prognostic factor for the prediction of disease outcome. Another study has shown that *PDCD4* suppresses tumor phenotype via inhibiting c-Jun and c-Fos activation in transformed (Tx) mouse epidermal JB6, RT101, cells.[15] It has also been reported that enforced expression of *PDCD4* inhibited tumorigenesis and malignant progression in K14-*PDCD4* transgenic mice.[8] However, it has also been shown that miR-21 can act as cooperative repressors of *PDCD4* in pancreatic ductal adenocarcinoma.[16]

MiR-21 is one of the most prominent microRNAs (miRNAs) implicated in the development and progression of different cancers, which has been shown to be involved in tumor progression,[17] proliferation[18] and with an anti-apoptotic effect[19] as well as its association with tumor resistance to chemotherapy.[20,21] There is a growing body of evidence showing miR-21 aberrant expression in CRC,[19,20,22] suggesting its value as a prognostic biomarker.[23,24]

Locked nucleic acid (LNA)-anti-miRs are a new class of modified oligonucleotides[25] that bind to miRNA and can modulate miRNA expression. They are very similar to RNAs, methylene bridge connecting the 2′-oxygen atom and the 4′-carbon atom (2′-O 4′-C methylene) in the ribose ring. This bridge forms a bi-cyclic structure that locks the ribose conformation and is integral to the high stability and low toxicity in biological systems and affinity of the LNA to its complementary RNA sequences.[26] LNA oligonucleotides are stable in the modulation of RNAs, have a good aqueous solubility, and do not cause an immune response, suggesting their value for antisense-based gene silencing in gene therapy.[23,27] Therefore, in the current study, we explored the anti-tumor activity of LNA-anti-miR-21 in colon adenocarcinoma cells and the modulation of *PDCD4* expression, through the analysis of cell migration and metastatic features of LS174T cells. This cell line is mucin-producing colorectal cell line mimicking the condition usually happens in younger patients with interference of high amounts of mucin in treatment effectiveness. The fact that mucin production hampers effective therapy remained obscure in previous works.

Materials and methods

Cell culture

The human colorectal adenocarcinoma cell line LS174T was obtained from the National Cell Bank of Iran (Pasteur Institute, Tehran, Iran) and was maintained in Dulbecco's modified Eagle's medium (DMEM; Gibco, Grand Island, NY, USA) with 4.5 g/L glucose, supplemented with 10% fetal bovine serum (FBS; Bio-IDEA, Tehran, Iran), 2-mM L-glutamine, 100 IU/mL penicillin, and 100 µg/mL streptomycin (Bio-IDEA). The cells were cultured to their exponential growth phase. LS174T cells were harvested using trypsin-EDTA and incubated at 37°C with 5% CO_2.

Cell transfection with LNA-anti-miR-21

Nucleotide sequences of miR-21 and related scientific data were obtained from a reputable site of www.mirbase.org. Human miR-21 has the accession number MIMAT0000076, with a sequence of nucleotides in the form of 5'- UAGCUUAUCAGACUGAUGUUGA-3'.

The inhibition interaction between miRNAs on mRNA *PDCD4* was obtained by using EMBL-EBI (MicroCosm Targets version 5), target scan program, and miRTarBase database. The LS174T cells were transfected with LNA-anti-miR-21, miRCURY LNA inhibitor (anti-miR), or scrambled LNA (Exiqon, Copenhagen, Denmark) using the X-tremeGENE siRNA Transfection Reagent Kit™ (Roche, Mannheim, Germany) according to the manufacturer's instructions. 5′ end of both nucleotides was marked with 6-carboxyfluorescein (6-FAM). Sequences of LNA-anti-miR-21 and scrambled LNA were as follows: 5′-3′/56-FAM/ACA TCA GTC TGA TAA GCT and 5′-3′/56-FAM/GTG TAA CAC GTC TAT ACG CCC A. The sequence of negative control was analyzed using BLAST search to exclude potential hits in the human transcriptome. Both oligonucleotides were purified by high-pressure liquid chromatography (HPLC). In brief, for cell transfection, 2×10^5 LS174T cells were cultured in each six-well culture plates (SPL Life Sciences, Pocheon, Korea), and plates were kept in a cell culture incubator in 37°C and 5% CO_2 for 24 h. For standard transfection, the culture medium was completely removed from each well and the cells were washed with phosphate-buffered saline (PBS; 1×) and serum-free medium for three times to decrease mucus layer on the cells, and subsequently, 1.8 mL of fresh medium containing 2.7% serum without antibiotics was added to each well containing cells. 2-µL of scrambled LNA or LNA-anti-miR (50 pmol/µL) was added separately with 5-µL X-tremeGENE siRNA transfection reagent in 200 µL Opti-MEMI (Gibco), followed by incubation in a dark room for 20 min at room temperature. The resulting complex was added to each well and slowly swirled while adding the complex to spread entirely in all parts of the plate. The plate was incubated for 10 h. Then, 200-µL FBS was added to each well, and the cells were incubated for 24, 48, and 72 h. The reverse transfection method was used for evaluation of cluster formation assay. In this method, LS174T cells were transfected in a state of suspension. Briefly, 4×10^5 cells were added to each well of 6-well low attachment plates (SPL Life Sciences), and subsequently, 1.8-mL DMEM with 2.7% FBS without antibiotics was added to each well. Transfection complexes of 200 µL were added to the cells. After 10 h, 200-µL 10% FBS was added to each well to maintain maximum viability.

Transfection efficiency was examined by fluorescence microscope (Olympus, Tokyo, Japan) and then analyzed by FACSCalibur flow cytometer (Becton-Dickinson Immunocytometry Systems, Franklin Lakes, NJ, USA).

Quantitative real-time polymerase chain reaction

Reverse transcriptase real-time polymerase chain reaction qRT-PCR was used to evaluate the efficiency of miR-21 inhibition by LNA-anti-miR-21 after 24, 48, and 72 h of transfection. Total RNA was extracted from LS174T cells after 24, 48, and 72 h of transfection by the miRCURY RNA Isolation Kit™ (Exiqon) according to the manufacturer's instructions. The concentration of RNA was measured using a NanoDrop Epoch (BioTek Instruments, Winooski, VT, USA). cDNA was synthesized by the Universal cDNA Synthesis Kit (Exiqon). Relative levels of miRNA were examined using the SYBR Green Master Mix Kit™ (Exiqon) with specific primers which hsa-miR-21-5p (Product No. 204230; Exiqon) and hsa-let-7a-5p (Product No. 205727; Exiqon)[28] as an internal control (Exiqon) to normalize quantitative real-time PCR (qRT-PCR). The relative miR-21 and let-7a expression were calculated using the ΔΔCT method. Moreover, for evaluation of *PDCD4* gene expression, total RNA was extracted as described above and cDNA was synthesized by the Fermentas kit (Fermentas Life Science, Vilnius, Lithuania) according to the manufacturer's instructions. qRT-PCR was performed using the SYBR® Green Master Mix Kit (Exiqon) according to the manufacturer's instructions. The primers' sequences for *PDCD4* were as follows: forward, 5′-AAAGGGAAGGTTGCTGGATAGG-3′; reverse, 5′-CACAGTTCTCCTGGTCATCATCA-3′. *GAPDH* was used as the internal control gene (forward, 5′-AGTCCA CTGGCGTCTTCAC-3′; reverse, 5′-AGGCATTGCTGAT GATCTTGAG-3′). The relative *PDCD4* and *GAPDH* expression were calculated using the ΔΔCT method. The StepOnePlus™ (Applied Biosystems, Foster City, CA, USA) instrument was used for real-time PCR experiments under the following conditions: polymerase activation at 95°C for 10 min followed by 40 cycles at 95°C for 10 s and 60°C for 1 min.

Western blot analysis

The level of protein expression of *PDCD4* was determined after 24, 48, and 72 h following transfection in the three groups of cells (transfected by LNA-anti-miR, transfected by scrambled LNA, and untreated cells) by using Western blot analysis. Total protein was extracted using RIPA (Radioimmunoprecipitation) lysis buffer (Santa Cruz Biotechnology, Santa Cruz, California, USA) containing RIPA, phenyl methyl sulfoxide (PMSF), sodium orthovanadate solution, and protease inhibitor cocktail solution. Protein concentrations were determined by the Quick Start™ Bradford Protein Assay Kit™ (Bio-Rad, Hercules, CA, USA). Electrophoresis was performed in discontinuous system of Laemmli[29] at 15°C in a vertical slab filled with electrophoresis buffer (25-Mm Tris, 192-mM glycine, and 0.1% sodium dodecyl sulfate (SDS), pH 8.3). Equal aliquots of solubilized total protein sample (100 µg per lane) were resolved on 12% polyacrylamide gel electrophoresis with 6% stacking gel. A prestained protein marker (9–170 kDa; CinnaGen, Tehran, Iran) was used to

estimate the molecular weight of proteins resolved by electrophoresis. Electrophoresis was applied with 20 mA per gel until the bromophenol blue had reached the separation gel. The current was then increased to 30 mA until the dye had migrated through the separation gel. Afterward, the gels were removed and the proteins were transferred onto the nitrocellulose membrane (Amersham, Piscataway, NJ, USA). The membranes were then blocked with buffer containing 5% skimmed milk (Sigma, St. louis, USA) and 0.05% Tween-20 (polyoxyethylene-20 sorbitan monolaurate)(Merck, Darmstadt, Germany) at 4°C. Mouse monoclonal antibody anti-human *PDCD4* (Santa Cruz Biotechnology) and mouse monoclonal antibody anti-human β-actin (Santa Cruz Biotechnology) were used at 1:200 dilution. The secondary antibody, horseradish peroxidase–conjugated goat anti-mouse IgG (Santa Cruz Biotechnology) was used at 1: 2000 dilutions. The position of the protein was visualized using diaminobenzidine (DAB; Sigma-Aldrich Company Ltd, Gillingham, UK) reagent. Results of densitometric analyses of Western blots were measured by ImageJ software ver. 1.42q (National Institute of Health, Bethesda, MD, USA). The β-actin was utilized as an internal control for normalization.

Scratch cell migration assay

For the migration assay, 2×10^5 cells/well were seeded into six-well plates (SPL Life Sciences) and grown to 90% confluence at 37°C with 5% CO_2. Then, culture medium on the cells was removed; cells were washed with PBS solution and exposed overnight in medium containing 0.5% serum. Afterward, a direct scratch on the bottom plate using three vertical scratches was created by using a sterilized glass rod with a sharp tip; the cells were gently washed with PBS to remove non-adherent cells separated from the plate's bottom area and replaced with 1.8 mL of fresh medium containing 2.7% FBS solution. After 24, 48, and 72 h following transfection in three groups of cells (transfected by LNA-anti-miR, transfected by scrambled LNA, and untreated cells), cell migration was evaluated by counting cells at 24, 48, and 72 h post transfection that migrated from the scratch edge. The average numbers of migratory cells in three random fields were counted at 200× magnification using an inverted light microscope (Nikon TS100, Tokyo, Japan).

Cluster-formation assay

For the cluster formation assay, cell suspensions were resuspended in DMEM supplemented with 2.7% FBS. 10h after reverse transfection, 2×10^4 cells were seeded into 24-well ultra-low attachment plates (Corning, Corning, NY, USA) and incubated at 37°C with 5% CO_2 for 48 h. Suspensions of cell clusters were transferred into six-well plates (SPL Life Sciences). After 24-h incubation at 37°C with 5% CO_2, cell clusters attached to the bottom of the plate for evaluation of biomass. The clusters were stained with cell stain solution (Cell Biolabs, San Diego, CA, USA) for 10 min and then washed with PBS. The average numbers of cells forming the cluster in three random fields were counted at 200× magnification using an inverted light microscope (Nikon TS100) in the three groups (transfected with LNA-anti-miR, scrambled LNA, and untreated cells).

In ovo experiments

To assess spontaneous metastasis, fertilized chicken eggs were randomly allocated to one of four groups: healthy chick embryos, scrambled LNA, LNA-anti-miR, and control (untreated cells). Fertilized chicken eggs were incubated in a rotating incubator at 38°C and 65% humidity for 10 days. Afterward, the air sac in the blunt end was determined using light source to candle the eggs. The chorioallantoic vein was detected and marked; 1-cm by 0.5-cm rectangle away from the area of capillary network connections was drawn with a pencil on the egg shell. Then, the area including blunt end and around the square was then cleaned using an iodine swab. A hole was made using a sterile pin in air sac and central part of the rectangle. Following suction made by the pump in the air sac, the new air pocket was formed under the drawn rectangle hole showing that chorioallantoic membrane (CAM) successfully separated from the egg shell. After CAM coming down, a small window above the rectangle, drawn on the egg shell, was removed with a sterile forceps. CAM was abraded using a cotton swab. A sterile plastic ring was placed on CAM area. All procedures were performed in accordance with the ethical standards of the local ethics committee of Mashhad University of Medical Sciences (permit number: 921797).

Chicken model for metastasis quantification

To study the metastatic features of tumor cells, burden in the livers of chicken embryo was determined by real-time quantitative PCR (qPCR) to detect human *Alu* repeats. *Alu* sequences are found in 500,000–1,000,000 copies in the haploid genome. They make an excellent target or marker for human DNA. After 48-h transfection, 10^5 cells were injected into an approximately 0.8-cm plastic ring placed on the 10-day-old chick CAM. After 8 days, the eggs were placed on ice for 3 h to anesthetize and euthanize. To assess metastasis, the livers were harvested and genomic DNA was extracted using the DNA Isolation Kit (Genet Bio, Cheonan, Korea). DNA concentration and purity were measured spectrophotometrically at an optical density (OD) of 260 to 280 nm with NanoDrop Epoch (BioTek). The concentration of genomic DNA extracted was regulated to 50 ng/μL. Genomic DNA was diluted 1:10 in nuclease-free water before using it in the subsequent PCR reaction for amplification. 1-μL diluted genomic DNA was

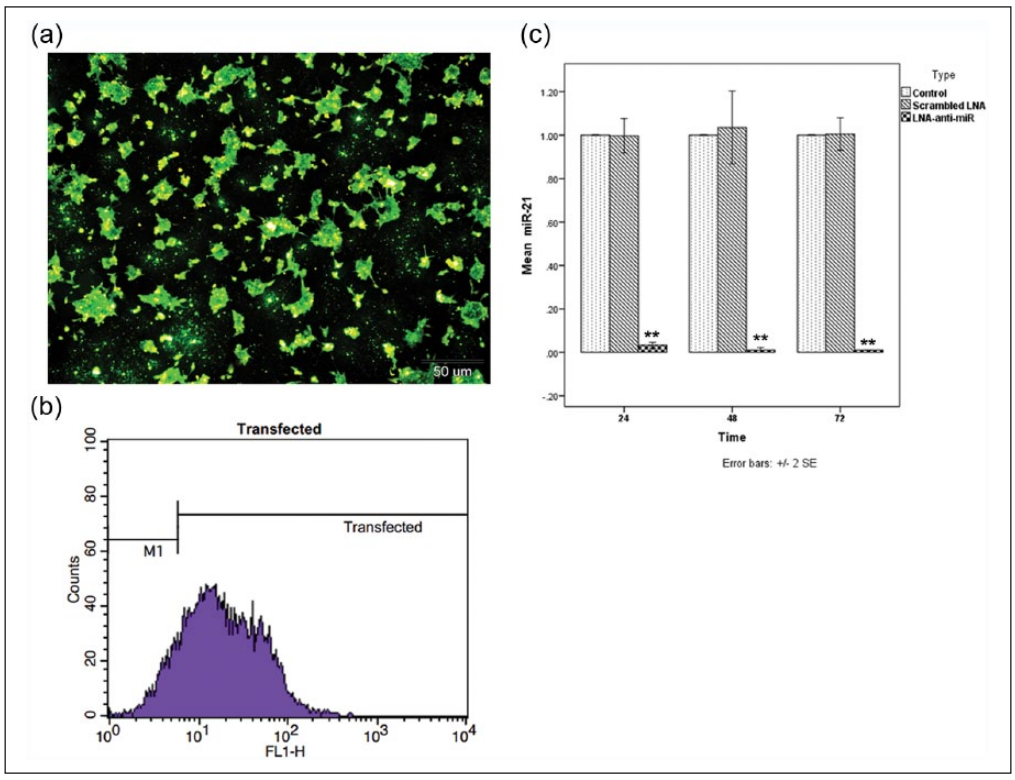

Figure 1. Transfection of LS174T cells. (a) LS174T cells were transfected with scrambled LNA 6-carboxyfluorescein (6-FAM)-labeled, as detected by fluorescent microscopy (×200); scale bars: 50μm; (b) fluorescence-activated cell sorting (FACS) analysis; (c) miR-21 expression after 24-, 48-, and 72-h transfection by qRT-PCR; data were mean ± 2SE of three independent experiments in the graph (**$p < 0.01$).

amplified in a total volume of 10-μL reaction, containing 1× RealQ Plus Master Mix Green (Ampliqon, Odense, Denmark), dH_2O, and 200 nmol/L of human *Alu* primers (*Alu*-F 5′-ACGCCTGTAATCCCAGCACTT-3′ and *Alu*-R 5′-TCGCCCAGGCTGGAGTGCA-3′) and chick glyceraldehyde-3-phosphate dehydrogenase (*chGAPDH*) specific primers (*chGAPDH*-F 5′-GAGGAAAGGTCGCCTGG TGGATCG-3′and *chGAPDH*-R 5′-GGTGAGGAC AAGCAGTGAGGAACG-3′) as endogenous controls. Metastasis was assessed using an ABI StepOnePlus™ instrument under the following conditions for *Alu* sequences: polymerase activation at 95°C for 15 min followed by 30 cycles at 95°C for 30 s, 63°C for 30 s, and 72°C for 30 s. Quantitative analysis by the ΔΔCT method for comparisons between groups was performed. Each assay included a negative control (no template controls, NTC), genomic DNA extracted from the liver of healthy chick embryos to determine the threshold between LS174T cells invaded and non-invaded cells.

Data analysis

The experiments were carried out in triplicate and repeated at least twice. Data were expressed as mean values ± standard deviation (SD) and analyzed by two-way analysis of variance (ANOVA) with Fisher's test followed by Scheffé's multiple comparisons test and compare means test-Dunnett. Data were analyzed using SPSS version 22 statistical software (IBM, Chicago, IL, USA). Statistical significance was set at **$p < 0.01$.

Results

LNA-anti-miR-21 reduced the expression of miR-21

We aimed to transfect the LS174T cells with FAM-labeled scrambled oligonucleotides (scrambled LNA group) to evaluate the transfection efficiency. Based on primary optimization experiments, different concentrations of the scrambled LNA were added to the cells and the transfection efficacy was assessed by fluorescence microscopy and flow cytometry. The best results were obtained at a concentration of 50 pmol of scrambled LNA and 5-μL X-tremeGENE siRNA transfection reagent. We found that the transfection efficacy was >85% (Figure 1(a) and (b)).

In order to see whether the target was inhibited, the expression level of miR-21 was evaluated by qRT-PCR after transfection for the 24, 48, and 72 h. This analysis revealed

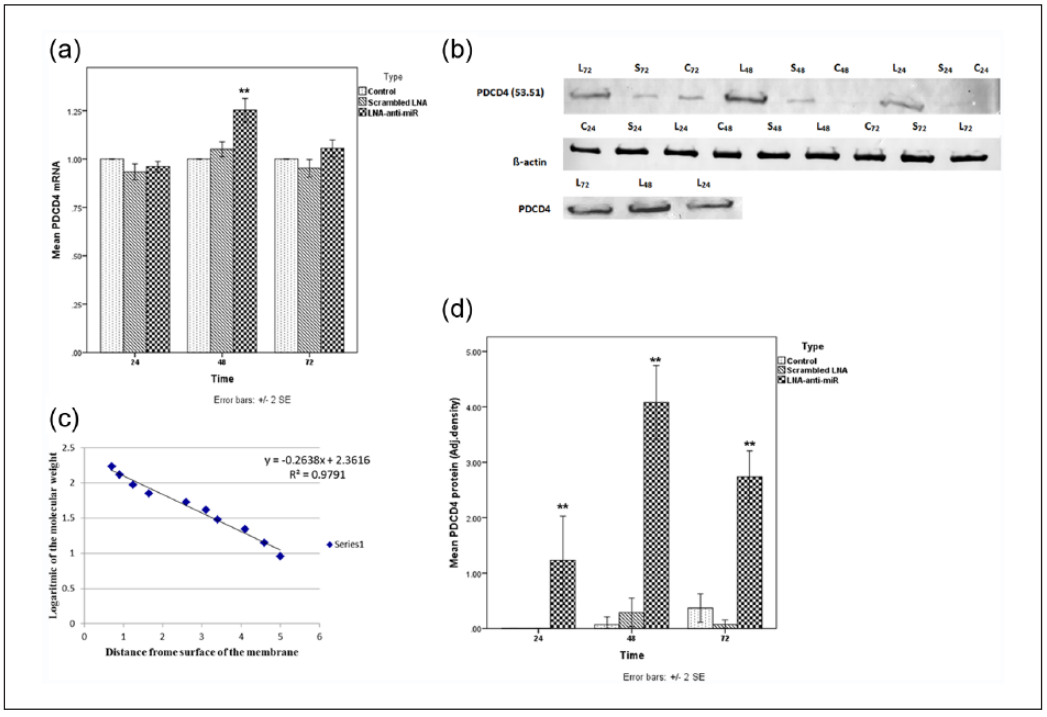

Figure 2. *PDCD4* expression. (a) The mRNA *PDCD4* level 24, 48, and 72 h after transfection was analyzed by qRT-PCR. The expression was normalized to *GAPDH*. Mean ± 2SE of three independent experiments in the graph (**$p < 0.01$). (b) Protein expression of *PDCD4* after 24-, 48-, and 72-h transfection as detected by Western blot analysis. The expression was normalized to beta-actin protein. (c) The regression curve was created with the distance from surface of the membrane and logarithmic of the molecular weight. (d) Density ratio of *PDCD4*/β-*actin* by Western blotting performed 24, 48, and 72 h after transfection; bar diagram, mean ± 2SE of three independent experiments in the graph (**$p < 0.01$).
L: LNA-anti-miR; S: scrambled LNA; C: untreated cells (control).

the downregulation of miR-21 in the LNA-anti-miR group. At all three time points, the expression of miR-21 was significantly lower in the LNA-anti-miR group compared with scrambled LNA and untreated groups (**$p < 0.01$; control: 1 ± 0.0, scrambled LNA: 1.01 ± 0.088, and LNA-anti-miR: 0.018 ± 0.013; Figure 1(c)).

LNA-anti-miR-21 modulated the PDCD4 *expression in LS174T cells*

The expression pattern of *PDCD4* was determined in cells before and after transfection with LNA-anti-miR-21 compared with scrambled LNA and untreated groups at mRNA and protein levels. We observed that the level of mRNA *PDCD4* was significantly increased at 48 h after transfection with LNA-anti-miR-21, although this effect was more pronounced after 72 h (Figure 2(a)). Notably, when LS174T cells were transfected with LNA-anti-miR, a significant increase in *PDCD4* mRNA expression levels was apparent compared with the control and scrambled LNA groups (**$p < 0.01$).

There was a statistically significant inverse correlation ($r = -0.502$; **$p < 0.01$) between miR-21 inhibition and *PDCD4* mRNA, which may be due to translational repression instead of mRNA degradation by miR-21 because an r indicates a weak correlation between the variables. We also evaluated the protein expression of *PDCD4* (Figure 2(b)). A strong inverse correlation was found between miR-21 inhibition and *PDCD4* protein ($r = -0.853$). The regression equation was used to evaluate the molecular weight with respect to the distance from the surface of membrane (Figure 2(c)). At all three time points, these data showed that the highest amount of *PDCD4* protein was associated to LNA-anti-miR-21-transfected cells (control: 0.16 ± 0.25, scrambled LNA: 0.14 ± 0.21, and LNA-anti-miR: 2.85 ± 1.37), and this effect was greater after 48 h.

After 24 h in the LNA-anti-miR-transfected cells, the expression level of *PDCD4* protein was increased, but in the untreated cells and cells transfected with scrambled LNA, *PDCD4* protein was not detected. At 24 h, this increasing pattern of *PDCD4* protein was continued at 48 h and decreased at 72 h after transfection, but this reduction was not less than that of 24 h after transfection (Figure 2(b)). In untreated and transfected cells treated with scrambled LNA, a very low level of *PDCD4* protein was detected after 48 and 72 h transfection that may be because of high expression of miR-21 in the cells that leads to significant translational repression instead of mRNA degradation (Figure 2(d)).

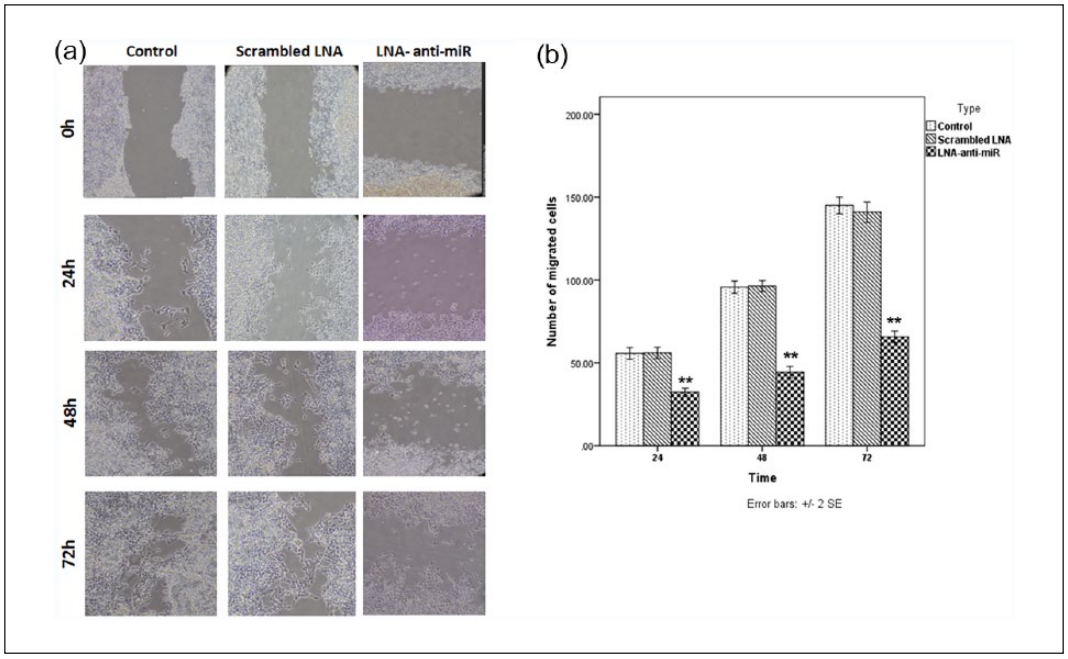

Figure 3. LNA-anti-miR-21 decreased cell migration. (a) Cell migration after 0, 24, 48, and 72 h in three groups: control, scrambled LNA, and LNA-anti-miR-transfected cells (magnification: ×200). (b) Different migration abilities of LS174T cells transfected with LNA-anti-miR compared with scrambled LNA–transfected cells and control groups in all three time points (**$p < 0.01$).

LNA-anti-miR-21 reduced cell migration

A cell scratch assay was performed to estimate the migratory behaviors of the cells after 24-, 48-, and 72-h transfection. This analysis showed that LNA-anti-miR-21 reduced the migratory properties of LS174T cells compared with scrambled LNA and untreated cells (Figure 3(a)). In addition, the average numbers of cells moved across the scraped edge were counted at 24, 48, and 72 h post transfection. The average number of LS174T cells transfected with LNA-anti-miR-21 that migrated for all three time points was 47.44 ± 14.82 cells per site. Notably, this average number was significantly lower than that for the scrambled LNA (97.77 ± 36.97 cells per site) and untreated (98.78 ± 38.87 cells per site) cells (Figure 3(b)).

LNA-anti-miR-21 decreased cluster-forming ability of LS174T cells

We investigated the effect of LNA-anti-miR-21 on cluster-forming ability of LS174T cells. The average number of cells forming the cluster was lower in the LS174T cells transfected by LNA-anti-miR-21 after 48-h transfection, compared with scrambled LNA and untreated cells. In particular, the average number of cells forming the cluster in transfected cells with LNA-anti-miR-21 was 20.67 ± 3.21, compared with 51.33 ± 1.53 cells per site for scrambled LNA and 50.0 ± 3.0 cells per site for untreated cells (Figure 4).

Inhibition of miR-21 reduced liver metastasis

LS174T cells were successfully grafted onto the CAM, outlined in Figure 5(a), to investigate the functional significance of metastasis in vivo assay. LS174T cells grafted CAM model were treated on day 10 with LNA-anti-miR-21, scrambled LNA, and untreated cells, exposed till day 18. After incubation, a primary tumor as the primary CAM tumor developed, allowing access to the chick vasculature for metastasis to more distant chick tissues. Then, livers were harvested and analyzed for metastases (Figure 5(b)). OD260/OD280 ratios of 1.4–1.8 were accepted to be adequate for qPCR for human *Alu* repeat sequences in DNA. The number of tumor cells in the liver was determined by comparison with a standard curve in which we plotted the qPCR signal for Alu repeats against known numbers of LS174T cells (Figure 6(a)). Interestingly, we observed no metastasis in embryos treated with LNA-anti-miR-21 (Figure 6(b)). Moreover, the average number of metastases was higher in the control group (2024.67 ± 1271.22 cells/sample) or scrambled LNA group (1490.33 ± 571.24 cells/sample) compared with the embryos treated with LNA-anti-miR-21 groups (0.05 ± 0.032 cells/sample; Figure 6(c)). Human genomic DNA was higher in the control group (0.41 ± 0.3 cells/sample) or scrambled LNA group (0.3 ± 0.13 cells/sample) compared with the embryos treated with LNA-anti-miR-21 groups (0.00 ± 0.00001 cells/sample; Figure 6(d)). However, cells treated with scrambled LNA or untreated cells had a significant higher rate of metastasis to liver.

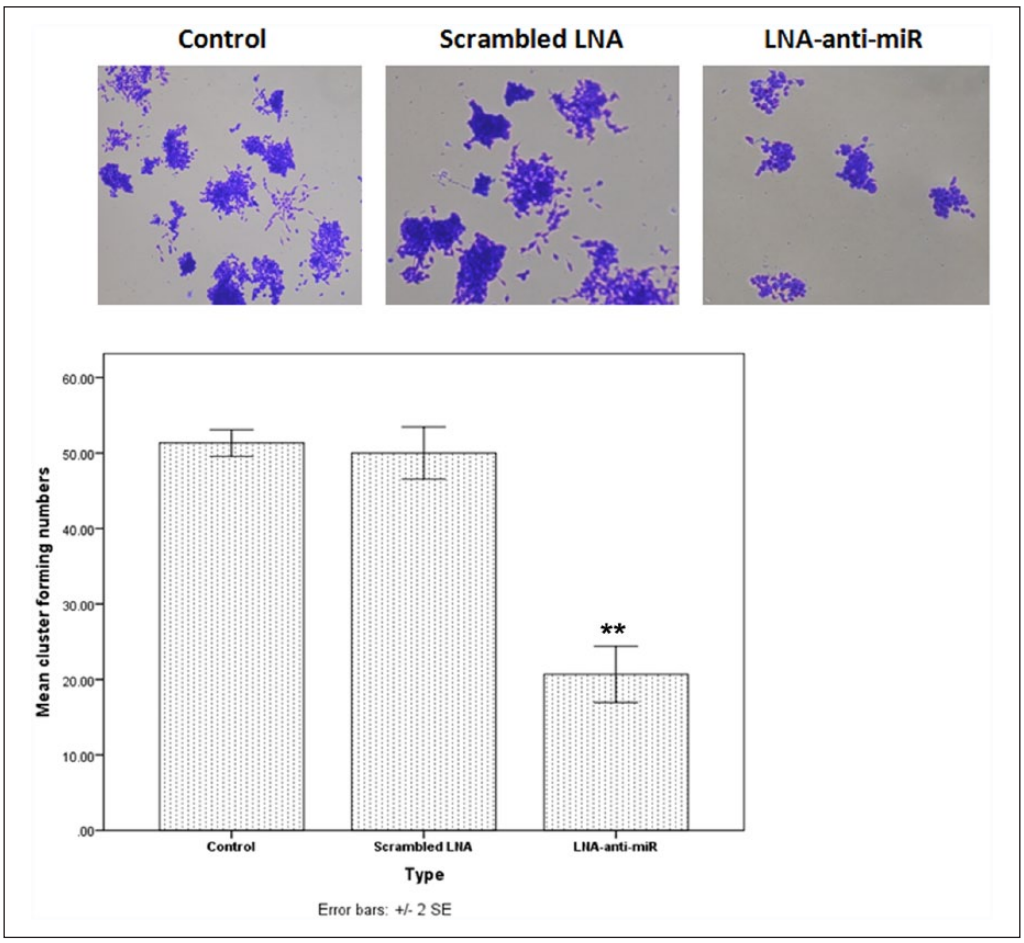

Figure 4. Transfection of the cells with LNA-anti-miR-21 decreased cluster-forming ability of LS174T cells. Different number of counted cells in each cluster transfected with LNA-anti-miR and scrambled LNA compared with control. In cells transfected with LNA-anti-miR, the cluster was significantly smaller compared with the other groups (**$p < 0.01$).

Discussion

To the best of our knowledge, this is the first study evaluating the inhibitory effect of LNA-anti-miR-21 and exploring its molecular mechanisms in vitro and in vivo, in the chick CAM model derived from human colorectal adenocarcinoma LS174T cells. Our results suggest that miR-21 expression could be of relevance to the critical biological behavior of colorectal neoplasia. We demonstrated that inhibition of miR-21 using novel LNA-anti-miR-21 suppressed its expression in human colorectal adenocarcinoma LS174T cells and reduced cell migration and liver metastasis in the CAM model, most likely through modulation of *PDCD4*.

There is mounting evidence showing the important role of miR-21 in different types of cancer, including CRC,[17,18,25,26,30–33] which has been suggested to be associated with poor prognosis and chemoresistance of CRC,[34,35] indicating its value as a potential therapeutic target. Furthermore, there appears to be an inverse correlation between miR-21 expression and *PDCD4* expression[15,36,37] which is in agreement with our data. It has also been documented that reduced expression of this tumor suppressor gene in CRCs is associated with poor prognosis.[13,15] In particular, Fassan et al.[36] evaluated *PDCD4* expression in 300 polypoid lesions of the colon mucosa (50 hyperplastic polyps, 50 serrated adenomas, 50 tubular adenomas with low-grade intraepithelial neoplasia, 50 tubular adenomas with high-grade intraepithelial neoplasia), 50 colon adenocarcinomas, and in 50 biopsy samples obtained from patients with irritable bowel syndrome as normal controls. They showed that miR-21 expression was upregulated in pre-neoplastic/neoplastic samples, consistent with *PDCD4* downregulation. Moreover, it has been reported that *PDCD4* could affect on tumor progression, malignant transformation, tumorigenesis,[8,15] and apoptosis.[38] Wei et al.[39] investigated the role and mechanism of miR-21 in promoting the 5-fluorouracil (5-FU) resistance of pancreatic cancer cells in 5-FU resistance cell line PATU8988/5-FU. They found that miR-21 regulated 5-FU drug resistance PATU8988 and PANC-1 cells via decreasing the expression of *PTEN* and *PDCD4*. In turn, enforced

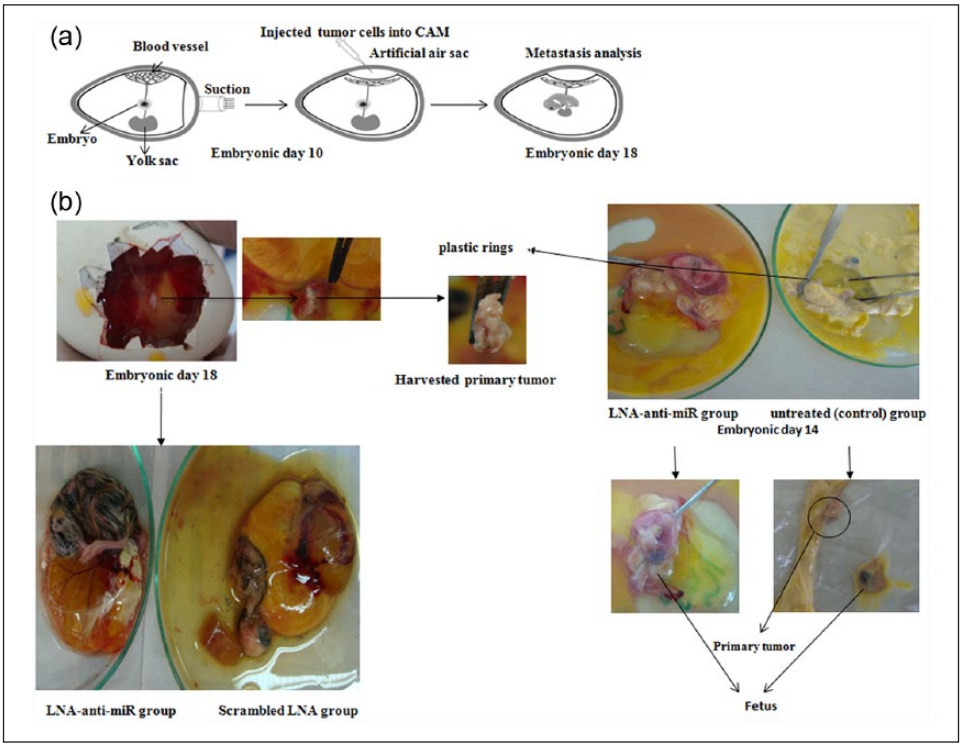

Figure 5. Inhibition of miR-21 reduced liver metastasis in CAM model. (a) Scheme of the spontaneous metastasis chick model. (b) The inhibition of spontaneous metastasis cells in a chick model treated with the LNA-anti-miR group compared with the untreated and scrambled LNA–treated cells groups. Cells were grafted in CAM at day 10; tumors and livers were harvested on day 18. MiR-21 knockdown by LNA-anti-miR-21 reduced metastasis of LS174T cells in the chick embryo spontaneous metastasis model.

expression of *PDCD4* attenuated the effects of miR-21 in 5-FU resistance cell line PATU8988/5-FU. Shi and colleagues[40] found that exosomal levels of miR-21 from cerebrospinal fluids were related with poor prognosis and tumor recurrence of glioma patients, whose expression was inversely correlated with *PDCD4* expression. A similar study also showed that the downregulation of *PDCD4* was correlated with aromatase inhibitor resistance and poor prognosis in estrogen receptor–positive breast cancer and forced overexpression of *PDCD4* resensitized aromatase-resistant cells to aromatase inhibitors or hormone deprivation.[41] Zhang et al.[42] have reported that modulation of miR-21 could affect on *PDCD4* in hepatocellular carcinoma.

These observations provide a proof of principle for the modulation of *PDCD4* expression via targeting miR-21 in CRC as a novel therapeutic option. Therefore, in this study, we investigated the inhibitory effects of LNA-anti-miR-21 in LS174T cells as a possible treatment for CRC. The LS174T cell line is able to produce large amounts of mucin and inhibit effective transfection.[43,44] At the optimized level, we found that transfection efficiency was more than 85%. This amount of transfection is considered to be important because one of the key challenges in the improvement of effective miRNA-based therapy is the delivery of stable and efficient agents into target cells.[45] Although the role of mucin in the behavior of colon cancer cells is not clear, other reports have suggested that mucinous adenocarcinoma is associated with a poorer outcome.[43] In addition, mucinous carcinoma has a higher incidence in the proximal colon and among younger patients than non-mucinous adenocarcinoma.[43] Our results showed that the expression of miR-21 was high, while the level of *PDCD4* protein was lower in LS174T cells before transfection with LNA-anti-miR-21. However, we found that *PDCD4* protein was markedly enhanced after transfection with LNA-anti-miR-21.

According to this study, miR-21 has a negative regulatory effect on *PDCD4* and it has anti-apoptotic effects.[38] LNA-anti-miR-21-transfected cells significantly increased *PDCD4* protein levels, but it almost caused weak alternations in *PDCD4* mRNA levels. These findings showed that miR-21 inhibits *PDCD4* protein production. It further suggests that miR-21 regulates *PDCD4* at the level of translational repression, instead of mRNA degradation. This finding strongly suggests that a high level of miR-21 expression in LS174T cells downregulated *PDCD4* protein expression at post-transcription level, and enhanced tumor cell invasion in vitro[38] and distant metastasis in vivo. Our findings showed that LNA-anti-miR-21 reduced cell migration and cluster-forming ability of LS174T cells. In particular, we successfully

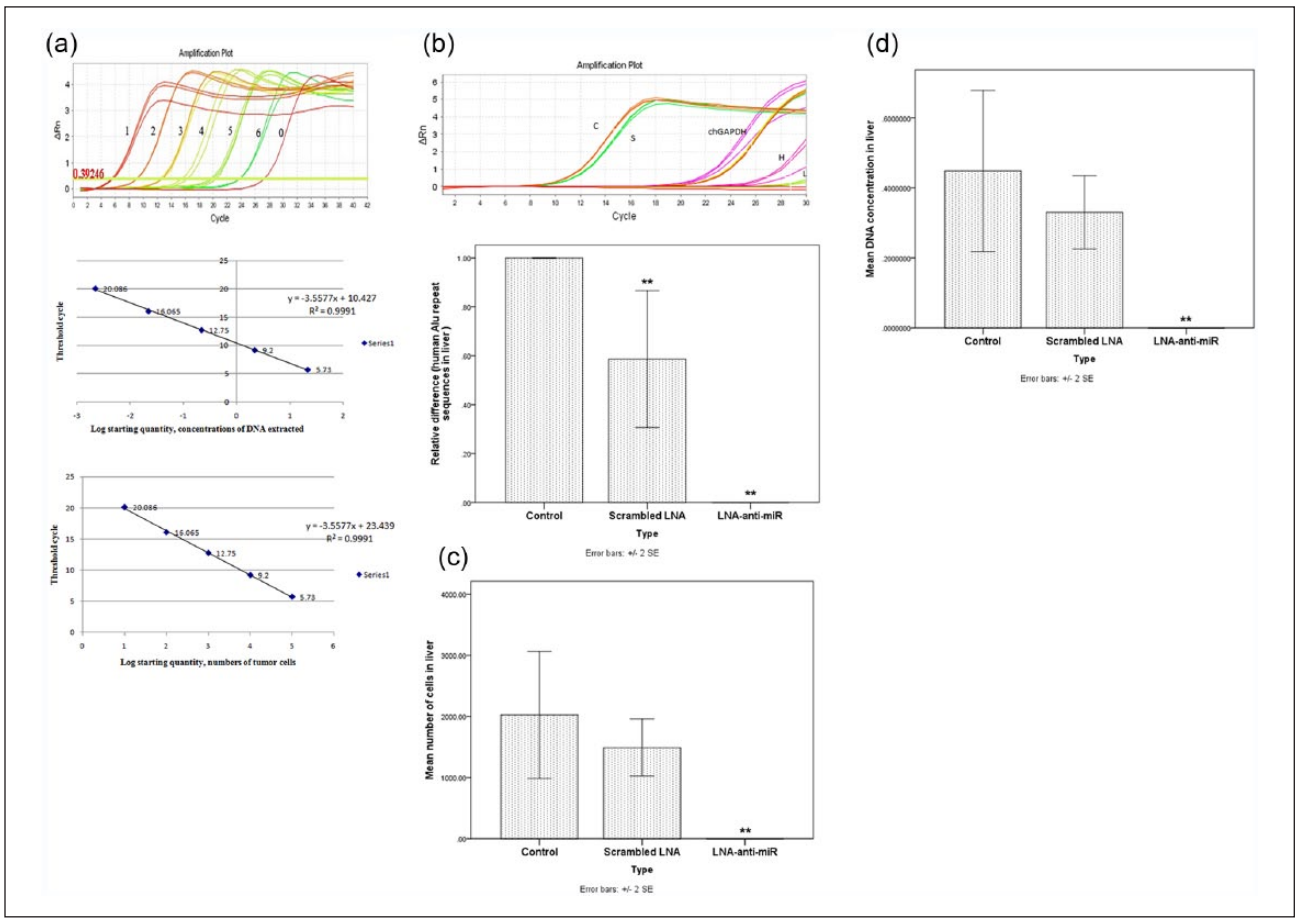

Figure 6. Validation of *Alu* PCR assays. (a) Human genomic DNA was extracted from LS174T cells, which had been serially diluted by 10-fold (lines 1, 22 ng/100,000 cells; lines 2, 2.2 ng/10,000 cells; lines 3, 0.22 ng/1000 cells; lines 4, 0.022 ng/100 cells; and lines 5, 0.00022 ng/10 cells), and then, *Alu* PCR was performed to detect human-specific *Alu* repeats in the liver lobes of chick embryo. The *Alu* standard curve was generated with the concentration of total DNA/numbers of tumor cells and threshold cycle of the 10-fold serially diluted human genomic DNA samples. These results were used to estimate the number of LS174T cells in liver by comparison with a standard curve. (b) The livers from each chick embryo were harvested 8 days later and subjected to quantitative real-time *Alu* PCR analysis. *chGAPDH* was used as an internal control. The ΔΔCT method was used for data analysis, and the untreated group was considered as a reference for each time point. Data were mean ± SD of three independent experiments (**$p < 0.01$). (c) Number of tumor cells metastasized to the liver was counted. Data were mean ± SD of three independent experiments (**$p < 0.01$). (d) Concentration of human genomic DNA metastasized to the liver was estimated. Data were mean ± 2SE of three independent experiments in the graph (**$p < 0.01$).

developed a CAM model using LS174T CRC cells. Also, the average number of tumor cells in the liver was significantly reduced in the eggs treated with LNA-anti-miR compared with the scrambled LNA and untreated cells. It seems that this performance is due to the effect of inhibiting the activity of matrix-metalloproteinase and inhibition of *u-PAR*, which is in agreement with several previous studies.[35,38,46–51]

Conclusion

Our study confirms that miR-21 triggers carcinogenic progression. Nowadays, miRNA-based therapeutic drug has moved to clinical trials, and it is possible to become a potential therapeutic target for cancers. In aggregate, our data illustrated that the inhibition of oncogenic role of miR-21 impairs the metastatic characteristic of colon adenocarcinoma cells, supporting further investigation on the therapeutic potential of LNA-anti-miR-21 as a new option for treatment of CRC.

Declaration of conflicting interests

The author(s) declared no potential conflicts of interest with respect to the research, authorship, and/or publication of this article.

Funding

This study was supported by the Mashhad University of Medical Sciences and Isfahan University of Medical Sciences (grant no. 921797).

References

1. Gong B, Liu WW, Nie WJ, et al. MiR-21/RASA1 axis affects malignancy of colon cancer cells via RAS pathways. *World J Gastroenterol* 2015; 21(5): 1488–1497.
2. Society AC. *Cancer facts & figures 2016*. Atlanta, GA: American Cancer Society, 2016.
3. Yu Y, Sarkar FH and Majumdar AP. Down-regulation of miR-21 induces differentiation of chemoresistant colon cancer cells and enhances susceptibility to therapeutic regimens. *Transl Oncol* 2013; 6(2): 180–186.
4. Lankat-Buttgereit B and Goke R. The tumour suppressor Pdcd4: recent advances in the elucidation of function and regulation. *Biol Cell* 2009; 101(6): 309–317.
5. Yang HS, Cho MH, Zakowicz H, et al. A novel function of the MA-3 domains in transformation and translation suppressor Pdcd4 is essential for its binding to eukaryotic translation initiation factor 4A. *Mol Cell Biol* 2004; 24(9): 3894–3906.
6. Zakowicz H, Yang HS, Stark C, et al. Mutational analysis of the DEAD-box RNA helicase eIF4AII characterizes its interaction with transformation suppressor Pdcd4 and eIF4GI. *RNA* 2005; 11(3): 261–274.
7. Goke R, Gregel C, Goke A, et al. Programmed cell death protein 4 (PDCD4) acts as a tumor suppressor in neuroendocrine tumor cells. *Ann N Y Acad Sci* 2004; 220–221.
8. Jansen AP, Camalier CE and Colburn NH. Epidermal expression of the translation inhibitor programmed cell death 4 suppresses tumorigenesis. *Cancer Res* 2005; 65(14): 6034–6041.
9. Lankat-Buttgereit B, Gregel C, Knolle A, et al. Pdcd4 inhibits growth of tumor cells by suppression of carbonic anhydrase type II. *Mol Cell Endocrinol* 2004; 214(1–2): 149–153.
10. Bitomsky N, Bohm M and Klempnauer KH. Transformation suppressor protein Pdcd4 interferes with JNK-mediated phosphorylation of c-Jun and recruitment of the coactivator p300 by c-Jun. *Oncogene* 2004; 23(45): 7484–7493.
11. Nieves-Alicea R, Colburn NH, Simeone A-M, et al. Programmed cell death 4 inhibits breast cancer cell invasion by increasing tissue inhibitor of metalloproteinases-2 expression. *Breast Cancer Res Treat* 2009; 114(2): 203–209.
12. Chen Y, Knosel T, Kristiansen G, et al. Loss of PDCD4 expression in human lung cancer correlates with tumour progression and prognosis. *J Pathol* 2003; 200(5): 640–646.
13. Mudduluru G, Medved F, Grobholz R, et al. Loss of programmed cell death 4 expression marks adenoma-carcinoma transition, correlates inversely with phosphorylated protein kinase B, and is an independent prognostic factor in resected colorectal cancer. *Cancer* 2007; 110(8): 1697–1707.
14. Chen X, Ba Y, Ma L, et al. Characterization of microRNAs in serum: a novel class of biomarkers for diagnosis of cancer and other diseases. *Cell Res* 2008; 18(10): 997–1006.
15. Yang HS, Knies JL, Stark C, et al. Pdcd4 suppresses tumor phenotype in JB6 cells by inhibiting AP-1 transactivation. *Oncogene* 2003; 22(24): 3712–3720.
16. Zhang Z and DuBois RN. Detection of differentially expressed genes in human colon carcinoma cells treated with a selective COX-2 inhibitor. *Oncogene* 2001; 20(33): 4450–4456.
17. Si M, Zhu S, Wu H, et al. miR-21-mediated tumor growth. *Oncogene* 2007; 26(19): 2799–2803.
18. Roldo C, Missiaglia E, Hagan JP, et al. MicroRNA expression abnormalities in pancreatic endocrine and acinar tumors are associated with distinctive pathologic features and clinical behavior. *J Clin Oncol* 2006; 24(29): 4677–4684.
19. Chan JA, Krichevsky AM and Kosik KS. MicroRNA-21 is an antiapoptotic factor in human glioblastoma cells. *Cancer Res* 2005; 65(14): 6029–6033.
20. Meng F, Henson R, Lang M, et al. Involvement of human micro-RNA in growth and response to chemotherapy in human cholangiocarcinoma cell lines. *Gastroenterology* 2006; 130(7): 2113–2129.
21. Zhu S, Si ML, Wu H, et al. MicroRNA-21 targets the tumor suppressor gene tropomyosin 1 (TPM1). *J Biol Chem* 2007; 282(19): 14328–14336.
22. Iorio MV, Ferracin M, Liu CG, et al. MicroRNA gene expression deregulation in human breast cancer. *Cancer Res* 2005; 65(16): 7065–7070.
23. Cowland JB, Hother C and Grønbæk K. MicroRNAs and cancer. *APMIS* 2007; 115(10): 1090–1106.
24. Hammond SM. MicroRNAs as oncogenes. *Curr Opin Genet Dev* 2006; 16(1): 4–9.
25. Orom UA, Kauppinen S and Lund AH. LNA-modified oligonucleotides mediate specific inhibition of microRNA function. *Gene* 2006; 372: 137–141.
26. Seto AG. The road toward microRNA therapeutics. *Int J Biochem Cell Biol* 2010; 42(8): 1298–1305.
27. Trang P, Weidhaas JB and Slack FJ. MicroRNAs as potential cancer therapeutics. *Oncogene* 2008; 27(2): 353.
28. Chang KH, Mestdagh P, Vandesompele J, et al. MicroRNA expression profiling to identify and validate reference genes for relative quantification in colorectal cancer. *BMC Cancer* 2010; 10(1): 1.
29. Laemmli UK. Cleavage of structural proteins during the assembly of the head of bacteriophage T4. *Nature* 1970; 227(5259): 680–685.
30. Slaby O, Svoboda M, Fabian P, et al. Altered expression of miR-21, miR-31, miR-143 and miR-145 is related to clinicopathologic features of colorectal cancer. *Oncology* 2008; 72(5–6): 397–402.
31. Yamamichi N, Shimomura R, Inada K, et al. Locked nucleic acid in situ hybridization analysis of miR-21 expression during colorectal cancer development. *Clin Cancer Res* 2009; 15(12): 4009–4016.
32. Kulda V, Pesta M, Topolcan O, et al. Relevance of miR-21 and miR-143 expression in tissue samples of colorectal carcinoma and its liver metastases. *Cancer Genet Cytogenet* 2010; 200(2): 154–160.
33. Wu CW, Ng SS, Dong YJ, et al. Detection of miR-92a and miR-21 in stool samples as potential screening biomarkers for colorectal cancer and polyps. *Gut* 2012; 61(5): 739–745.
34. Valeri N, Gasparini P, Braconi C, et al. MicroRNA-21 induces resistance to 5-fluorouracil by down-regulating human DNA MutS homolog 2 (hMSH2). *Proc Natl Acad Sci USA* 2010; 107(49): 21098–21103.
35. Asangani IA, Rasheed SA, Nikolova DA, et al. MicroRNA-21 (miR-21) post-transcriptionally downregulates tumor suppressor Pdcd4 and stimulates invasion, intravasation and metastasis in colorectal cancer. *Oncogene* 2008; 27(15): 2128–2136.

36. Fassan M, Pizzi M, Giacomelli L, et al. PDCD4 nuclear loss inversely correlates with miR-21 levels in colon carcinogenesis. *Virchows Arch* 2011; 458(4): 413–419.
37. George GP and Mittal RD. MicroRNAs: potential biomarkers in cancer. *Indian J Clin Biochem* 2010; 25(1): 4–14.
38. Nedaeinia R, Sharifi M, Avan A, et al. Locked nucleic acid anti-miR-21 inhibits cell growth and invasive behaviors of a colorectal adenocarcinoma cell line: lNA-anti-miR as a novel approach. *Cancer Gene Ther* 2016; 23(8): 246–253.
39. Wei X, Wang W, Wang L, et al. MicroRNA-21 induces 5-fluorouracil resistance in human pancreatic cancer cells by regulating PTEN and PDCD4. *Cancer Med* 2016; 5(4): 693–702.
40. Shi R, Wang P-Y, Li X-Y, et al. Exosomal levels of miRNA-21 from cerebrospinal fluids associated with poor prognosis and tumor recurrence of glioma patients. *Oncotarget* 2015; 6(29): 26971–26981.
41. Chen Z, Yuan Y-C, Wang Y, et al. Down-regulation of programmed cell death 4 (PDCD4) is associated with aromatase inhibitor resistance and a poor prognosis in estrogen receptor-positive breast cancer. *Breast Cancer Res Treat* 2015; 152(1): 29–39.
42. Zhang N, Duan WD, Leng JJ, et al. STAT3 regulates the migration and invasion of a stem-like subpopulation through microRNA-21 and multiple targets in hepatocellular carcinoma. *Oncol Rep* 2015; 33(3): 1493–1498.
43. Bu X, Li L, Li N, et al. Suppression of mucin 2 enhances the proliferation and invasion of LS174T human colorectal cancer cells. *Cell Biol Int* 2011; 35(11): 1121–1129.
44. Klinkspoor JH, Mok KS, Van Klinken BJ-W, et al. Mucin secretion by the human colon cell line LS174T is regulated by bile salts. *Glycobiology* 1999; 9(1): 13–19.
45. Mirnezami AH, Pickard K, Zhang L, et al. MicroRNAs: key players in carcinogenesis and novel therapeutic targets. *Eur J Surg Oncology* 2009; 35(4): 339–347.
46. Allgayer H. Pdcd4, a colon cancer prognostic that is regulated by a microRNA. *Crit Rev Oncol Hematol* 2010; 73(3): 185–191.
47. Huang Y, Yang YB, Zhang XH, et al. MicroRNA-21 gene and cancer. *Med Oncol* 2013; 30(1): 012–0376.
48. Najafi Z, Sharifi M and Javadi G. Degradation of miR-21 induces apoptosis and inhibits cell proliferation in human hepatocellular carcinoma. *Cancer Gene Ther* 2015; 22(11): 530–535.
49. Schmid T, Jansen AP, Baker AR, et al. Translation inhibitor Pdcd4 is targeted for degradation during tumor promotion. *Cancer Res* 2008; 68(5): 1254–1260.
50. Sharifi M, Salehi R, Gheisari Y, et al. Inhibition of microRNA miR-92a induces apoptosis and inhibits cell proliferation in human acute promyelocytic leukemia through modulation of p63 expression. *Mol Biol Rep* 2014; 41(5): 2799–2808.
51. Shen L, Wan Z, Ma Y, et al. The clinical utility of microRNA-21 as novel biomarker for diagnosing human cancers. *Tumor Biol* 2015; 36(3): 1993–2005.